

LHC constraints on $M_{1/2}$ and m_0 in the semi-constrained NMSSM

Debottam Das¹, Ulrich Ellwanger¹ and Ana M. Teixeira²

¹ *Laboratoire de Physique Théorique, UMR 8627, CNRS and Université de Paris-Sud, Bât. 210, 91405 Orsay, France*

² *Laboratoire de Physique Corpusculaire, CNRS/IN2P3 – UMR 6533, Campus des Cézeaux, 24 Av. des Landais, F-63171 Aubière Cedex, France*

Abstract

Constraints from searches for squarks and gluinos at the LHC at $\sqrt{s}=8$ TeV are applied to the parameter space of the NMSSM with universal squark/slepton and gaugino masses at the GUT scale, but allowing for non-universal soft Higgs mass parameters (the sNMSSM). We confine ourselves to regions of the parameter space compatible with a 125 GeV Higgs boson with diphoton signal rates at least as large as the Standard Model ones, and a dark matter candidate compatible with WMAP and XENON100 constraints. Following the simulation of numerous points in the $m_0 - M_{1/2}$ plane, we compare the constraints on the sNMSSM from 3-5 jets + missing E_T channels as well as from multijet + missing E_T channels with the corresponding cMSSM constraints. Due to the longer squark decay cascades, lower bounds on $M_{1/2}$ are alleviated by up to 50 GeV. For heavy squarks at large m_0 , the dominant constraints originate from multijet + missing E_T channels due to gluino decays via stop pairs.

1 Introduction

One of the most important tasks of the LHC – besides the quest for the Higgs boson – is the search for new elementary particles like those predicted in supersymmetric (SUSY) extensions of the Standard Model (SM). So far the search for such SUSY particles (sparticles) has not been successful; the absence of corresponding signal events can be interpreted as lower bounds on sparticle masses (see [1–6] for recent ATLAS publications of results at $\sqrt{s}=8$ TeV, [7–11] for recent CMS publications of results at $\sqrt{s}=8$ TeV, [12] and the web pages [13] and [14] for summaries of searches for sparticles by the ATLAS and CMS collaboration). Clearly these lower bounds on sparticle masses are not model independent, since they depend on the sparticle couplings and decay cascades, and hence on a large number of unknown parameters.

The large number of unknown parameters of SUSY extensions of the SM is greatly reduced if one assumes universal soft SUSY breaking terms at the Grand Unification (GUT) scale, which is also theoretically appealing. Such models are denoted as “constrained”, and this is the case of the cMSSM (constrained Minimal Supersymmetric extension of the SM). Since the various sparticle masses and couplings are now strongly correlated, constrained models often serve as useful benchmark scenarios. The bounds on sparticle masses can then be represented as bounds in the $m_0 - M_{1/2}$ plane, where m_0 denotes the universal squark and slepton masses and $M_{1/2}$ the universal gaugino masses at the GUT scale. Frequently the cMSSM with $\tan\beta = 10$ and $A_0 = 0$ is used to this end ($\tan\beta$ being the ratio of the two Higgs vevs $\langle H_u \rangle / \langle H_d \rangle$, and A_0 denoting the universal soft SUSY breaking trilinear couplings at the GUT scale).

However, most of the considered parameter space of the cMSSM with $\tan\beta = 10$ and $A_0 = 0$ is neither consistent with the observation of a SM like Higgs boson near 125 GeV [15,16], nor with the dark matter relic density as determined by the WMAP experiment [17]. In recent publications [18–24], the LHC bounds on sparticle masses have been applied to the cMSSM (or variants thereof as the NUHM with non-universal soft Higgs masses at the GUT scale), but with parameters consistent with a SM like Higgs boson near 125 GeV, and/or dark matter consistent with WMAP bounds on the relic density and XENON100 limits [25] on the dark matter direct detection cross section. Generally, one finds that the bounds on sparticle masses obtained within variants of the cMSSM or in the NUHM are similar to the cMSSM with $\tan\beta = 10$ and $A_0 = 0$.

The MSSM is not the only possible supersymmetric extension of the SM. The simplest supersymmetric extension of the Standard Model with a scale invariant superpotential, i.e. where the soft SUSY breaking terms are the only dimensionful parameters, is the Next-to-Minimal Supersymmetric Standard Model (NMSSM) [26]. A supersymmetric Higgs mass term μ , as required in the MSSM, is generated dynamically by a vacuum expectation value (vev) of a gauge singlet (super-)field S , and is naturally of the order of the SUSY breaking scale. The attractive features of the MSSM are preserved, like a solution of the hierarchy problem, the unification of the running gauge coupling constants at a Grand Unification scale, and a dark matter candidate in the form of a stable lightest SUSY particle (LSP).

The additional coupling λ of the Higgs bosons in the NMSSM makes it much easier to accommodate a SM like Higgs boson near 125 GeV [27–50] and alleviates the corresponding “little fine-tuning problem” of the cMSSM since lighter scalar top quarks (top squarks) are

possible [27–29, 31–33, 35, 36, 39–42, 44, 46, 48, 49, 51]. The fermionic component of the gauge singlet superfield \hat{S} extends the neutralino sector of the MSSM, and this can lead to more complicated sparticle cascade decays [34, 52–56].

Like in the MSSM, one can consider constrained versions of the NMSSM with universal soft SUSY breaking terms at the GUT scale. A SM like Higgs boson near 125 GeV can easily be obtained within the semi-constrained NMSSM in which, similar to the NUHM, the soft SUSY breaking Higgs mass terms (and the trilinear couplings involving the singlet S) are allowed to deviate from the soft SUSY breaking terms involving squarks or sleptons. In several recent publications the parameter space of the semi-constrained NMSSM compatible with a SM like Higgs boson near 125 GeV (and possibly an enhanced diphoton signal rate) has been discussed [30, 35, 38, 45, 57]. The LHC constraints from negative squark and gluino searches had to be estimated or had been left aside, unless trivially satisfied due to very heavy squarks and/or gluinos. LHC constraints from the runs at $\sqrt{s} = 7$ TeV, using the razor variables at CMS [58], have been studied within a more restricted version of the semi-constrained NMSSM allowing *only* the soft SUSY breaking singlet mass term to deviate from m_0 in [59]. In this case the regions in the parameter space corresponding to large λ , low m_0 and $M_{1/2}$, which are interesting from the point of view of a 125 GeV Higgs with low fine-tuning, are not viable.

Hence it becomes interesting and important to re-analyse the LHC constraints on sparticle masses within the semi-constrained NMSSM, which is the purpose of the present paper. We focus on the most constraining squark and gluino search channels analysed by the ATLAS collaboration for the $\sqrt{s} = 8$ TeV run: Searches for final states with jets and missing transverse momentum [4], final states with large jet multiplicities [1], and with an isolated lepton [2].

We confine ourselves to phenomenologically acceptable regions of the sNMSSM parameter space with a Higgs boson near 125 GeV, a diphoton signal rate near or above its SM value, a dark matter relic density in agreement with WMAP constraints, and a dark matter direct detection cross section compatible with XENON100 constraints. The latter constrain the neutralino sector (the mass and the couplings of the lightest SUSY particle, the LSP) which has some impact on the sparticle decay cascades.

In the NMSSM, sparticle decay cascades can differ from the MSSM for various reasons:

- The higgsino-like neutralinos and charginos can be lighter than in most realistic scenarios within the MSSM (with a Higgs boson near 125 GeV and a dark matter relic density compatible with WMAP constraints). The additional singlet-like neutralino (singlino) can mix with the MSSM like neutralinos, implying more complicated sparticle cascade decays [34, 52–56].
- The top squarks are typically lighter than in realistic scenarios within the cMSSM (with a Higgs boson near 125 GeV), implying gluino/squark cascade decays via top squarks which lead to multijet events, reducing the missing transverse momentum and the average transverse momenta of jets.

Hence it is not clear to which extent the bounds in the $m_0 - M_{1/2}$ plane obtained by ATLAS for the cMSSM with $\tan\beta = 10$ and $A_0 = 0$ are applicable to the semi-constrained NMSSM; the results of our present study allow to answer this question quantitatively.

In the next section, we briefly review the semi-constrained NMSSM and discuss our choice for points in the $m_0 - M_{1/2}$ plane. In Section 3 we describe the tools used for the Monte Carlo studies and list the applied LHC constraints. In Section 4 we present the resulting bounds in the $m_0 - M_{1/2}$ and $M_{\text{squark}} - M_{\text{gluino}}$ planes, discuss the origin of the differences in the bounds within the semi-constrained NMSSM with respect to the cMSSM, and summarise our conclusions.

2 The semi-constrained NMSSM

The NMSSM differs from the MSSM due to the presence of the gauge singlet superfield \hat{S} . In the simplest realisation of the NMSSM, the $\mu\hat{H}_u\hat{H}_d$ Higgs mass term in the MSSM superpotential W_{MSSM} is replaced by the coupling λ of \hat{S} to \hat{H}_u and \hat{H}_d , and a self-coupling $\kappa\hat{S}^3$. Hence, in this version the superpotential W_{NMSSM} is scale invariant, and given by:

$$W_{\text{NMSSM}} = \lambda\hat{S}\hat{H}_u \cdot \hat{H}_d + \frac{\kappa}{3}\hat{S}^3 + \dots, \quad (1)$$

where the dots denote the Yukawa couplings of \hat{H}_u and \hat{H}_d to the quarks and leptons as in the MSSM. Once the scalar component of \hat{S} develops a vev s , the first term in W_{NMSSM} generates an effective μ -term with

$$\mu_{\text{eff}} = \lambda s. \quad (2)$$

The soft SUSY breaking terms consist of mass terms for the Higgs bosons H_u, H_d, S , squarks $\tilde{q}_i \equiv (\tilde{u}_{iL}, \tilde{d}_{iL}), \tilde{u}_{iR}^c, \tilde{d}_{iR}^c$ and sleptons $\tilde{\ell}_i \equiv (\tilde{\nu}_{iL}, \tilde{e}_{iL})$ and \tilde{e}_{iR}^c (where $i = 1 \dots 3$ is a generation index):

$$-\mathcal{L}_0 = m_{H_u}^2 |H_u|^2 + m_{H_d}^2 |H_d|^2 + m_S^2 |S|^2 + m_{\tilde{q}_i}^2 |\tilde{q}_i|^2 + m_{\tilde{u}_i}^2 |\tilde{u}_{iR}^c|^2 + m_{\tilde{d}_i}^2 |\tilde{d}_{iR}^c|^2 + m_{\tilde{\ell}_i}^2 |\tilde{\ell}_i|^2 + m_{\tilde{e}_i}^2 |\tilde{e}_{iR}^c|^2, \quad (3)$$

trilinear interactions involving the third generation squarks, sleptons and the Higgs fields (neglecting the Yukawa couplings of the first two generations):

$$-\mathcal{L}_3 = \left(h_t A_t Q \cdot H_u \tilde{u}_{3R}^c + h_b A_b H_d \cdot Q \tilde{d}_{3R}^c + h_\tau A_\tau H_d \cdot L \tilde{e}_{3R}^c + \lambda A_\lambda H_u \cdot H_d S + \frac{1}{3} \kappa A_\kappa S^3 \right) + \text{h.c.}, \quad (4)$$

and mass terms for the gauginos \tilde{B} (bino), \tilde{W}^a (winos) and \tilde{G}^a (gluinos):

$$-\mathcal{L}_{1/2} = \frac{1}{2} \left[M_1 \tilde{B} \tilde{B} + M_2 \sum_{a=1}^3 \tilde{W}^a \tilde{W}_a + M_3 \sum_{a=1}^8 \tilde{G}^a \tilde{G}_a \right] + \text{h.c.} \quad (5)$$

The neutral CP-even Higgs sector contains 3 states H_i , which are mixtures of the CP-even components of the superfields \hat{H}_u, \hat{H}_d and \hat{S} . Their masses are described by a 3×3 mass matrix \mathcal{M}_{Hij}^2 . The neutral CP-odd Higgs sector contains 2 physical states A_i , whose masses are described by a 2×2 mass matrix \mathcal{M}_{Aij}^2 . In the neutralino sector we have 5

states χ_i^0 , which are mixtures of the bino \widetilde{B} , the neutral wino \widetilde{W}^3 , the neutral higgsinos from the superfields \hat{H}_u and \hat{H}_d , and the singlino from the superfield \hat{S} . Their masses are described by a 5×5 mass matrix $\mathcal{M}_{\chi^0 ij}$. Expressions for the mass matrices – after H_u , H_d and S have developed vevs v_u , v_d and s , and including the dominant radiative corrections – can be found in [26] and will not be repeated here.

As compared to two independent parameters in the Higgs sector of the MSSM at tree level (often chosen as $\tan \beta$ and M_A), the Higgs sector of the NMSSM contains six parameters

$$\lambda, \kappa, A_\lambda, A_\kappa, \tan \beta \equiv v_u/v_d, \mu_{\text{eff}}; \quad (6)$$

then the soft SUSY breaking mass terms for the Higgs bosons $m_{H_u}^2$, $m_{H_d}^2$ and m_S^2 are determined implicitly by M_Z , $\tan \beta$ and μ_{eff} .

In constrained versions of the NMSSM (as in the constrained MSSM) one assumes that the soft SUSY breaking terms involving gauginos, squarks and sleptons are universal at the GUT scale:

$$M_1 = M_2 = M_3 \equiv M_{1/2}, \quad (7)$$

$$m_{\tilde{q}_i}^2 = m_{\tilde{u}_i}^2 = m_{\tilde{d}_i}^2 = m_{\tilde{\ell}_i}^2 = m_{\tilde{e}_i}^2 \equiv m_0^2, \quad (8)$$

$$A_t = A_b = A_\tau \equiv A_0. \quad (9)$$

In the semi-constrained NMSSM considered here, one allows the Higgs sector to play a special rôle: the Higgs soft mass terms $m_{H_u}^2$, $m_{H_d}^2$ and m_S^2 are allowed to differ from m_0^2 (and determined implicitly as noted above), and the trilinear couplings A_λ , A_κ can differ from A_0 . Hence the complete parameter space is characterised by

$$\lambda, \kappa, \tan \beta, \mu_{\text{eff}}, A_\lambda, A_\kappa, A_0, M_{1/2}, m_0, \quad (10)$$

where the latter five parameters are taken at the GUT scale.

Subsequently we are interested in regions of the parameter space with large NMSSM-specific contributions to the SM-like Higgs mass, i.e. large values of λ (and κ) and low values of $\tan \beta$, which lead naturally to a SM-like Higgs boson H_2 in the 125 GeV range [27–50]. We impose constraints from LEP [60] on the lighter mostly singlet-like Higgs boson H_1 , which still allow for a H_1 mass below 114 GeV if its coupling to the Z boson is reduced. For H_2 we require $124 \text{ GeV} < M_{H_2} < 127 \text{ GeV}$, $\sigma_{\text{obs}}^{\gamma\gamma}(H_2)/\sigma_{\text{SM}}^{\gamma\gamma} > 1$ and $\sigma_{\text{obs}}^{ZZ}(H_2)/\sigma_{\text{SM}}^{ZZ} \sim 1$ in order to comply with the observations at the LHC.

We have implemented these constraints into a modified version of the public code NMSPEC [61] inside NMSSMTools [62, 63]. (In the Higgs sector we have used two-loop radiative corrections from [64], and for the top quark pole mass we have taken $m_{\text{top}} = 173.1 \text{ GeV}$.) The constraints from B -physics are those of the version 3.2.0 of NMSSMTools, which are easily satisfied for the regime $\tan \beta < 3$ relevant here. The dark matter relic density and direct detection cross section of the LSP χ_1^0 (the lightest neutralino) are computed by MicrOmegas [65–67] implemented in NMSSMTools. However, due to the low values of $\tan \beta$, the SUSY contribution to the anomalous magnetic moment of the muon Δa_μ is not large enough to resolve the discrepancy between the SM and its measured value.

Leaving aside Δa_μ , many regions in the space of the parameters in (10) satisfy all the above conditions. Hence we proceed as follows: We start with a “lattice” in the $m_0 - M_{1/2}$

plane, i.e. numerous fixed values for m_0 and $M_{1/2}$. For each fixed $(m_0, M_{1/2})$ we choose the remaining parameters such that not only the above phenomenological constraints are satisfied, but also in such a way that the lighter top squark mass and μ_{eff} are relatively small.

Light stop quarks and low μ_{eff} minimise the fine-tuning [27–29, 31–33, 35, 36, 39–42, 44, 46, 48, 49, 51]. On the other hand, present constraints from searches for these sparticles should be satisfied. First, since gluinos with masses below ~ 1 TeV are excluded, constraints from gluino mediated stop production [5, 7, 68, 69] turn out to be satisfied. Constraints from direct pair production of top squarks \tilde{t} [6, 70–74] require $m_{\tilde{t}_1} \gtrsim 400$ GeV for LSP masses of ~ 80 GeV, as found below (note that slightly stronger bounds assume branching ratios and neutralino/chargino masses within simplified models which are not valid here; see [75] for proposals for search strategies for light stops within the general NMSSM). In addition, we require $\mu_{\text{eff}} \gtrsim 120$ GeV so that the lighter chargino masses and chargino-neutralino mass splittings comply with present constraints.

For each such point on a lattice in the $m_0 - M_{1/2}$ plane, we perform Monte Carlo simulations ($\sim 10^4$ events), apply the cuts described in the next section, and compare the resulting signal event numbers to present constraints. This allows to identify viable regions (up to error bars) in the $m_0 - M_{1/2}$ and $M_{\text{squark}} - M_{\text{gluino}}$ planes within the semi-constrained NMSSM.

3 Monte Carlo simulation, search channels and verification

For the calculation of the matrix elements we use MadGraph/MadEvent 5 [76], which includes Pythia 6.4 [77] for showering and hadronisation. Matching of the differential jet cross sections is performed according to the prescriptions in [78]. The sparticle branching ratios are obtained with the help of the code NMSDECAY [79] (based on SDECAY [80]), and are passed to Pythia.

The output is given in StdHEP-format to the fast detector simulation Delphes [81]. Inside Delphes, the anti-k(t) jet reconstruction algorithm [82] is used, with the jet reconstruction performed by FastJet [83].

The sparticle (squark and gluino) production cross sections are obtained by Prospino at next-to-leading order (NLO) [84–86]. The resummation of soft gluon emission is taken into account in the form of a correction factor estimated from [87], and the theoretical uncertainties from scale and PDF choices are obtained from [87, 88].

To the output from Delphes we apply cuts on final states with jets and missing transverse momentum from searches for supersymmetry at $\sqrt{s} = 8$ TeV with an integrated luminosity of 5.8 fb^{-1} by the ATLAS collaboration [4], which give at present the strongest constraints in the $m_0 - M_{1/2}$ plane in the cMSSM, as well as cuts on final states with large jet multiplicities from [1] and one isolated lepton from [2] which could, a priori, be relevant for the NMSSM.

In Table 1 we summarise the cuts corresponding to the search channels which lead to the most stringent constraints in the $m_0 - M_{1/2}$ plane in the semi-constrained NMSSM (depending on m_0 and $M_{1/2}$), and the 95% confidence level (CL) upper limits (UL) on

Channel	C-tight [4]	D-tight [4]	E-tight [4]	9j55 [1]	8j80 [1]
N_{jet}	4	5	6	≥ 9	≥ 8
$E_T^{\text{miss}} >$	160	160	160		
$E_T^{\text{miss}}/\sqrt{H_T} >$				4	4
$p_T(j_1) >$	130	130	130	55	80
$p_T(j_2 \dots j_{N_{jet}}) >$	60	60	60	55	80
$m_{\text{eff}}(\text{incl.}) >$	1900	1700	1400		
$E_T^{\text{miss}}/m_{\text{eff}}(N_j) >$	0.25	0.15	0.15		
95% CL UL on N_{SE}	3.3	6.0	9.3	5.4	4.0

Table 1: Cuts and 95% CL upper limits on the number N_{SE} of signal events at $\sqrt{s} = 8$ TeV and 5.8 fb^{-1} integrated luminosity for the search channels leading to the most stringent constraints in the $m_0 - M_{1/2}$ plane in the cMSSM or the semi-constrained NMSSM. (E_T^{miss} , p_T , H_T and m_{eff} in GeV.)

the number N_{SE} of signal events beyond the expected background in the corresponding channels, for an integrated luminosity of 5.8 fb^{-1} . (More details on the event selections can be found in [1, 4]; bounds from the searches including one isolated lepton did not lead to stronger constraints.) Here $m_{\text{eff}}(N_j)$ is the scalar sum of the transverse momenta of E_T^{miss} together with the leading N jets, $m_{\text{eff}}(\text{incl.})$ the scalar sum of the transverse momenta of E_T^{miss} together with all jets with $p_T > 40$ GeV, and H_T the scalar sum of the transverse momenta of all jets with $p_T > 40$ GeV without E_T^{miss} .

We first verified the validity of our simulations in the framework of the cMSSM with $\tan\beta = 10$ and $A_0 = 0$: For points in the $m_0 - M_{1/2}$ plane along the 95% CL exclusion line in [4] we determined the number of signal events in all search channels, divided them by the corresponding upper limits given in [4], and computed a ratio R from the most constraining search channel (giving the largest value for R). If our simulations would coincide exactly with those in [4], we would obtain $R = 1$. The resulting ratio R is shown as function of m_0 in Figure 1, where we also indicate the most constraining search channel by colours: black (full) for C-tight, blue (dashed) for D-tight and green (dotted) for E-tight. The most constraining search channels, depending on m_0 , coincide with the information given in [4].

We see that R deviates from 1 by up to $\pm 30\%$, which we take as uncertainty in the number of signal events after cuts due to our simulation (it is considerably larger than our statistical error). This error is added linearly to the error on production cross sections from scale and PDF choices (which are slightly squark and gluino mass dependent). For a given value of m_0 we determine three different values of $M_{1/2}$: one such that the number of signal events in the sNMSSM coincides with the 95% CL UL in Table 1 (for the most constraining channel), and two more such that the number of signal events in the sNMSSM coincides with the 95% CL UL \pm the relative error obtained as before. This leads to an exclusion curve in the $m_0 - M_{1/2}$ plane, as well as to curves which represent our errors on the number of signal events.

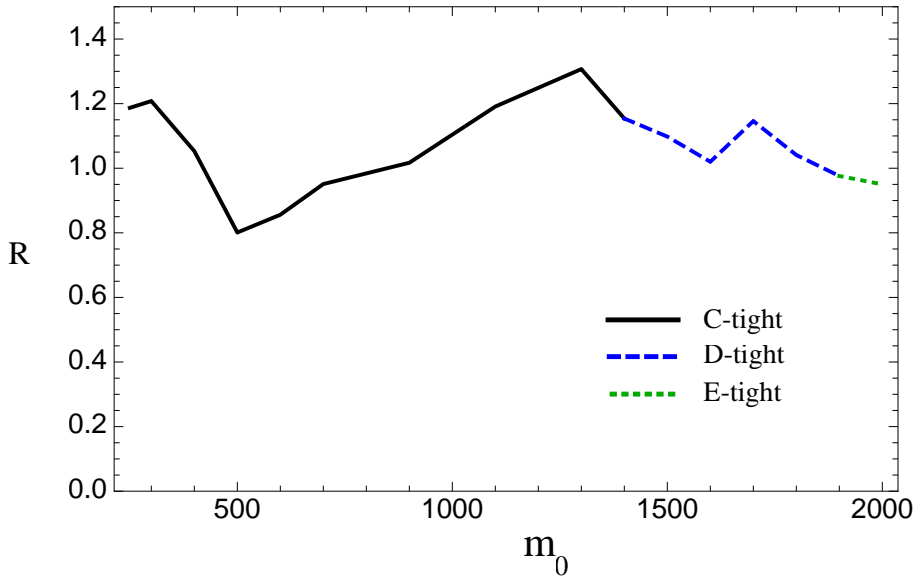


Figure 1: The ratio R of the number of signal events N_{SE} from our simulation within the cMSSM along the 95% CL exclusion line in [4], divided by the upper limits given in Table 1 from [4]. The colours indicate the most constraining search channel: black (full) for C-tight, blue (dashed) for D-tight and green (dotted) for E-tight.

4 Results and discussion

After simulation of a variety of points in the $m_0 - M_{1/2}$ plane in the semi-constrained NMSSM and application of the cuts, we require that accepted points give a number of signal events below the 95% CL upper limit in each search channel, \pm the uncertainty as determined above. This procedure generates the bounds in the $m_0 - M_{1/2}$ plane shown in Fig. 2, together with the uncertainties indicated by dashed lines. (The colours in Fig. 2 indicate the most constraining search channels: red for the jets + E_T^{miss} channels C-tight, D-tight or E-tight from [4], and blue for the multijet + E_T^{miss} channels 9j55 or 8j80 from [1].)

Note that, for a given value of m_0 , the upper and lower error lines can originate from different search channels. For comparison, we also show the bounds obtained by ATLAS for the cMSSM with $\tan\beta = 10$ and $A_0 = 0$ as a black line.

We see that for lower values of m_0 , the cMSSM bounds are alleviated due to NMSSM specific sparticle decay cascades. For larger values of m_0 the bounds within the semi-constrained NMSSM seem stronger. This is due to the fact that in this regime bounds from the multijet channels [1] become stronger than the bounds from the otherwise dominant channel E-tight; notice that the bounds from the multijet channels [1] are not included in the ATLAS bounds for the cMSSM with $\tan\beta = 10$ and $A_0 = 0$ from [4]. We have verified that the bounds from the multijet channels [1] would also dominate in the cMSSM for $m_0 \gtrsim 1400$ GeV, leading to cMSSM bounds somewhat stronger than those given in [4].

The corresponding bounds in the $M_{\text{squark}} - M_{\text{gluino}}$ plane are shown in Fig. 3. Here the region $m_0 \lesssim 1500$ GeV ($M_{1/2} \gtrsim 450$ GeV), where the bounds from the jets +

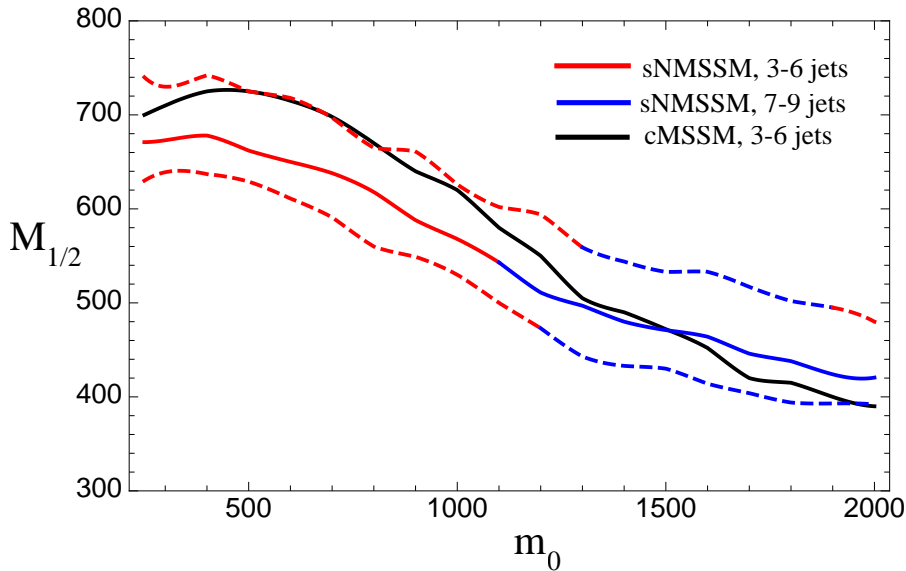


Figure 2: Bounds in the $m_0 - M_{1/2}$ plane in the semi-constrained NMSSM (dashed lines indicate our error bars), and ATLAS bounds for the cMSSM with $\tan\beta = 10$ and $A_0 = 0$ from [4] in black. The colours indicate the most constraining search channel for the NMSSM: Red for the jets + E_T^{miss} channels C-tight, D-tight or E-tight from [4], and blue for the multijet + E_T^{miss} channels 9j55 or 8j80 from [1].

E_T^{miss} channels are somewhat weaker in the sNMSSM than in the cMSSM, corresponds to $M_{\text{squark}} \lesssim 1700$ GeV ($M_{\text{gluino}} \gtrsim 1200$ GeV).

The different cMSSM and sNMSSM bounds are due to having distinct sparticle decay cascades. In the following, we discuss these cascades (which depend on m_0) in more detail.

For $m_0 \lesssim 1000$ GeV, the sparticle production cross section is dominated by up/down squark pair production. In the cMSSM with $\tan\beta = 10$ and $A_0 = 0$, the μ -parameter and hence the higgsino masses are relatively large (≈ 800 GeV), the binos and winos are approximately eigenstates with masses $\sim 0.4 \times M_{1/2}$, $\sim 0.8 \times M_{1/2}$, respectively, and the bino is the LSP (violating generally WMAP bounds on the relic density). The dominant decays of the right-handed squarks \tilde{q}_R and left-handed squarks \tilde{q}_L are

$$\tilde{q}_R \rightarrow q + \chi_1^0; \quad \tilde{q}_L \rightarrow q + \chi_1^\pm \rightarrow q + W^\pm + \chi_1^0, \quad (11)$$

where χ_1^0 is essentially bino-like and χ_1^\pm essentially wino-like. Hence the dominant decay cascades are relatively short.

In the semi-constrained NMSSM with a SM-like Higgs mass of ~ 125 GeV and a dark matter relic density consistent with WMAP constraints, the effective μ -parameter (and hence the higgsino masses), as well as the singlino mass parameter $2\kappa s$, are relatively small, in the 115 – 250 GeV range. Apart from alleviating the “little fine-tuning problem”, such higgsino and singlino mass parameters generate large mixing angles in the neutralino sector.

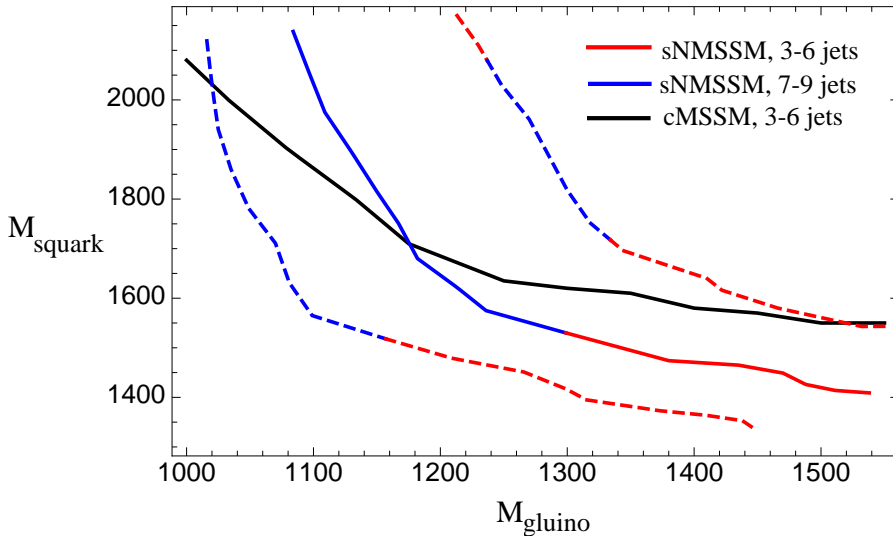


Figure 3: Bounds in the $M_{\text{squark}} - M_{\text{gluino}}$ plane in the semi-constrained NMSSM (dashed lines indicate our error bars), and ATLAS bounds for the cMSSM with $\tan\beta = 10$ and $A_0 = 0$ from [4] in black. Colour/line code as in Fig. 2.

The LSP, the lightest neutralino, is a mixture of higgsinos and singlino. The mostly bino-like neutralino is χ_4^0 , i.e. not the LSP, and the lighter chargino χ_1^\pm is essentially higgsino-like. Hence the dominant decays of the right-handed and left-handed squarks are

$$\tilde{q}_R \rightarrow q + \chi_4^0 \rightarrow q + W^\mp + \chi_1^\pm \rightarrow q + W^\mp + W^{\pm*} + \chi_1^0 ; \quad (12)$$

$$\tilde{q}_L \rightarrow q + \chi_2^\pm \rightarrow q + Z/H + \chi_1^\pm \rightarrow q + Z/H + W^{\pm*} + \chi_1^0 . \quad (13)$$

The squark decay cascades lead to considerably more final states in the NMSSM, implying less missing transverse momentum and less p_T per jet compared to the cMSSM. This explains the lower number of signal events, and the somewhat lower bound in the $m_0 - M_{1/2}$ plane. An example for a benchmark point with these properties (with $m_0 = 600$ GeV and $M_{1/2} = 650$ GeV) is given in Table 2.

For m_0 close to 250 GeV (and $M_{1/2} \lesssim 800$ GeV), another phenomenon appears in the semi-constrained NMSSM with a SM like Higgs mass of ~ 125 GeV: The Higgs mass requires a non-universal soft Higgs mass term m_{H_u} , which is considerably larger than m_0 at the GUT scale. This has some impact on the running squark and notably on the slepton masses from the GUT to the weak scale, leading to light sleptons. In fact, the LEP2 bound on light slepton masses of ~ 100 GeV leads to a lower bound $m_0 \gtrsim 250$ GeV on the parameter space. Moreover, the mostly bino-like neutralino decays dominantly into sleptons in this region. We have checked that constraints from searches in the channels including isolated leptons in [2] are satisfied in this region, and the dominant constraints still originate from the channel C-tight.

For $m_0 \gtrsim 1000$ GeV, the sparticle production cross section becomes dominated by squark-gluino production and, for $m_0 \gtrsim 1400$ GeV, by gluino pair production. In the cMSSM, gluinos undergo three-body decays involving virtual squarks, with some preference

$\lambda (M_{\text{SUSY}})$	0.64	M_{H_1}	123	Decays	BR(%)
$\kappa (M_{\text{SUSY}})$	0.36	M_{H_2}	125	$\tilde{u}_L \rightarrow \chi_5^0 + u$	31
$\tan \beta (M_{\text{SUSY}})$	3.02	M_{H_3}	377	$\tilde{u}_L \rightarrow \chi_2^+ + d$	62
$\mu_{\text{eff}} (M_{\text{SUSY}})$	120	$R_2^{\gamma\gamma}$ (ggF)	1.73	$\tilde{d}_L \rightarrow \chi_5^0 + d$	32
$M_{1/2}$	650	R_2^{ZZ} (ggF)	1.05	$\tilde{d}_L \rightarrow \chi_2^- + u$	65
m_0	600	$M_{\chi_1^0}$ (LSP)	76.5	$\tilde{u}_R \rightarrow \chi_4^0 + u$	94
A_0	-1262	\tilde{H}_d comp. of χ_1^0	0.49	$\tilde{d}_R \rightarrow \chi_4^0 + d$	94
A_λ	-426	\tilde{H}_u comp. of χ_1^0	0.72	$\chi_4^0 \rightarrow \chi_1^\pm + W^\mp$	69
A_κ	-176	\tilde{S} comp. of χ_1^0	0.43	$\chi_4^0 \rightarrow \chi_1^0 + H_1$	18
$\langle M_{\text{squarks } \tilde{u}, \tilde{d}} \rangle$	1425	$M_{\chi_2^0}$	159	$\chi_5^0 \rightarrow \chi_1^\pm + W^\mp$	45
M_{gluino}	1490	$M_{\chi_3^0}$	196	$\chi_5^0 \rightarrow \chi_2^0 + Z$	17
$M_{\tilde{t}_1}$	604	$M_{\chi_4^0}$ (bino)	283	$\chi_5^0 \rightarrow \chi_1^0 + H_1$	15
Ωh^2	0.0941	$M_{\chi_1^\pm}$ (higgsino)	112	$\chi_1^\pm \rightarrow \chi_1^0 + W^*$	100
σ_{SI}^p	8.4×10^{-10}	$M_{\chi_5^0}, M_{\chi_2^\pm}$ (winos)	540	$\chi_2^\pm \rightarrow \chi_1^\pm + Z$	23
				$\chi_2^\pm \rightarrow \chi_1^\pm + H_1$	20
				$\chi_2^\pm \rightarrow \chi_1^0 + W^\pm$	21
				$\chi_2^\pm \rightarrow \chi_2^0 + W^\pm$	17

Table 2: Input parameters, spectrum and some branching fractions of a benchmark point with $m_0 = 600$ GeV, $M_{1/2} = 650$ GeV. All dimensionful quantities are given in GeV. σ_{SI}^p denotes the spin independent LSP-proton cross section, for which the present XENON100 bound is $\lesssim 3 \times 10^{-9}$ for a LSP mass of $\simeq 77$ GeV. $R_2^{\gamma\gamma}$, R_2^{ZZ} denote the signal cross sections of H_2 relative to the SM, which are given in the gluon fusion production mode (ggF). The reduced signal cross sections of H_1 in these channels are about 0.25. $\tilde{H}_{u,d}$ and \tilde{S} denote the higgsino and the singlino components of χ_1^0 , respectively.

for the somewhat lighter squarks of the third generation. In the semi-constrained NMSSM, the non-universal soft Higgs mass term m_{H_u} , as well as the larger value for the top Yukawa coupling h_t (due to the lower value of $\tan \beta$), lead to lighter stop masses. Apart from alleviating the “little fine-tuning problem”, such stop masses imply dominant gluino two-body decays into the top quark + the lighter top squark (practically 100%). The latter decays dominantly into a bottom quark + the lighter chargino. (As discussed above, we verify that present bounds from top squark searches are satisfied.) Hence the final states involve a large number of jets, but a somewhat reduced missing transverse momentum. Whereas many of these final states would pass the cuts in the searches for jets and missing transverse momentum in [4], the searches for large jet multiplicities in [1] become now more relevant and, in fact, the constraints from the multijet channel are now dominant. For this reason, the constraints for $m_0 \gtrsim 1400$ GeV in the semi-constrained NMSSM are stronger than those from the channels D-tight and E-tight on the cMSSM in [4]. This would not be the case if the constraints from the multijet channel would be applied to the cMSSM. A second benchmark point with these properties (with $m_0 = 1900$ GeV and $M_{1/2} = 450$ GeV) is given in Table 3.

$\lambda (M_{\text{SUSY}})$	0.61	M_{H_1}	95
$\kappa (M_{\text{SUSY}})$	0.37	M_{H_2}	126
$\tan \beta (M_{\text{SUSY}})$	2.31	M_{H_3}	331
$\mu_{\text{eff}} (M_{\text{SUSY}})$	126	$R_2^{\gamma\gamma}$ (ggF)	1.78
$M_{1/2}$	450	R_2^{ZZ} (ggF)	1.40
m_0	1900	$M_{\tilde{\chi}_1^0}$ (LSP)	79
A_0	-875	\tilde{H}_d comp. of $\tilde{\chi}_1^0$	0.54
A_λ	-296	\tilde{H}_u comp. of $\tilde{\chi}_1^0$	0.68
A_κ	-385	\tilde{S} comp. of $\tilde{\chi}_1^0$	0.32
$\langle M_{\text{squarks } \tilde{u}, \tilde{d}} \rangle$	2070	$M_{\tilde{\chi}_2^0}$	162
M_{gluino}	1140	$M_{\tilde{\chi}_3^0}$	192
$M_{\tilde{t}_1}$	555	$M_{\tilde{\chi}_4^0}$ (bino)	212
Ωh^2	0.105	$M_{\tilde{\chi}_1^\pm}$ (higgsino)	109
σ_{SI}^p	7.2×10^{-9}	$M_{\tilde{\chi}_3^0}, M_{\tilde{\chi}_2^\pm}$ (winos)	398

Decays	BR(%)
$\tilde{g} \rightarrow \tilde{t}_1 + t$	100
$\tilde{t}_1 \rightarrow \tilde{\chi}_1^+ + b$	51
$\tilde{t}_1 \rightarrow \tilde{\chi}_1^0 + t$	22
$\tilde{t}_1 \rightarrow \tilde{\chi}_2^0 + t$	18
$\tilde{\chi}_2^0 \rightarrow \tilde{\chi}_1^0 + Z^*$	79
$\tilde{\chi}_2^0 \rightarrow \tilde{\chi}_1^\pm + W^*$	20
$\tilde{\chi}_1^\pm \rightarrow \tilde{\chi}_1^0 + W^*$	100

Table 3: Input parameters, spectrum and some branching fractions of a benchmark point with $m_0 = 1900$ GeV, $M_{1/2} = 450$ GeV. The reduced signal cross sections of H_1 in the channels bb , $\gamma\gamma$ and ZZ (in the gluon fusion production mode) are ~ 0.025 .

We conclude that the present bounds on m_0 and $M_{1/2}$ in the semi-constrained NMSSM with a SM like Higgs mass of ~ 125 GeV are somewhat alleviated with respect to the cMSSM for $m_0 \lesssim 1000$ GeV (mostly for $m_0 \sim 500$ GeV) due to the longer and more complicated sparticle decay cascades. This phenomenon could have been anticipated. Here we have studied it concretely with the result that the lower bound on $M_{1/2}$, at fixed m_0 , decreases by at most 50 GeV for $m_0 \sim 500$ GeV; for $m_0 \gtrsim 1100$ GeV ($M_{\text{squark}} \gtrsim 1500$ GeV), the lower bound arises from multijet searches, whereas those of the cMSSM were derived from jet and missing transverse momentum search channels. The central line in Fig. 2 serves to compare the bounds to the cMSSM whereas, to be conservative, the lower dashed line including our uncertainties should be used for bounds in the $m_0 - M_{1/2}$ plane in the semi-constrained NMSSM. Moreover it is likely that, within the general NMSSM (as in the phenomenological MSSM in [23]), lower bounds on sparticle masses are much weaker. We expect that a large variety of corresponding scenarios are possible within the general NMSSM, which will require more dedicated studies.

Acknowledgements

UE acknowledges partial support from the French ANRs STR-COSMO and LFV-CPV-LHC, and UE and AMT from the European Union FP7 ITN INVISIBLES (Marie Curie Actions, PITN-GA-2011-289442). DD thanks the Department of Theoretical Physics, Indian Association for the Cultivation of Science (IACS), and Harish-Chandra Research Institute (HRI), Allahabad for kind hospitality during the final stages of this work.

References

- [1] ATLAS Collaboration, “Search for new phenomena using large jet multiplicities and missing transverse momentum with ATLAS in 5.8 fb^{-1} of $\sqrt{s}=8 \text{ TeV}$ proton-proton collisions”, ATLAS-CONF-2012-103
- [2] ATLAS Collaboration, “Search for supersymmetry at $\sqrt{s}=8 \text{ TeV}$ in final states with jets, missing transverse momentum and one isolated lepton”, ATLAS-CONF-2012-104
- [3] ATLAS Collaboration, “Search for Supersymmetry in final states with two same-sign leptons, jets and missing transverse momentum with the ATLAS detector in pp collisions at $\sqrt{s}=8 \text{ TeV}$, ATLAS-CONF-2012-105
- [4] ATLAS Collaboration, “Search for squarks and gluinos with the ATLAS detector using final states with jets and missing transverse momentum and 5.8 fb^{-1} of $\sqrt{s}=8 \text{ TeV}$ proton-proton collision data”, ATLAS-CONF-2012-109
- [5] ATLAS Collaboration, “Search for supersymmetry using events with three leptons, multiple jets, and missing transverse momentum in 13.0 fb^{-1} of pp collisions with the ATLAS detector at $\sqrt{s}=8 \text{ TeV}$ ”, ATLAS-CONF-2012-151
- [6] ATLAS Collaboration, “Search for direct stop production in events with missing transverse momentum and two b-jets using 12.8 fb^{-1} of pp collisions at $\sqrt{s} = 8 \text{ TeV}$ with the ATLAS detector”, ATLAS-CONF-2013-001
- [7] CMS Collaboration, “Search for supersymmetry in final states with missing transverse momentum and 0, 1, 2, or ≥ 4 b jets in 8 TeV pp collisions”, CMS-PAS-SUS-12-016
- [8] CMS Collaboration, “Search for supersymmetry in events with same-sign dileptons”, CMS-PAS-SUS-12-017
- [9] CMS Collaboration, “Search for supersymmetry in events with photons and missing energy”, CMS-PAS-SUS-12-018
- [10] CMS Collaboration, “Search for direct top squark pair production in events with a single isolated lepton, jets and missing transverse energy at $\sqrt{s} = 8 \text{ TeV}$ ”, CMS-PAS-SUS-12-023
- [11] CMS Collaboration, “Search for supersymmetry in final states with missing transverse energy and 0, 1, 2, or ≥ 4 b jets in 8 TeV pp collisions”, CMS-PAS-SUS-12-028
- [12] P. de Jong, “Supersymmetry searches at the LHC,” ATL-PHYS-PROC-2012-244, arXiv:1211.3887 [hep-ex].
- [13] <https://twiki.cern.ch/twiki/bin/view/AtlasPublic/SupersymmetryPublicResults>
- [14] <https://twiki.cern.ch/twiki/bin/view/CMSPublic/PhysicsResultsSUS>
- [15] G. Aad *et al.* [ATLAS Collaboration], Phys. Lett. B **716** (2012) 1 [arXiv:1207.7214 [hep-ex]].

- [16] S. Chatrchyan *et al.* [CMS Collaboration], Phys. Lett. B **716** (2012) 30 [arXiv:1207.7235 [hep-ex]].
- [17] E. Komatsu *et al.* [WMAP Collaboration], Astrophys. J. Suppl. **192** (2011) 18 [arXiv:1001.4538 [astro-ph.CO]].
- [18] P. Bechtle, T. Bringmann, K. Desch, H. Dreiner, M. Hamer, C. Hensel, M. Kramer and N. Nguyen *et al.*, JHEP **1206** (2012) 098 [arXiv:1204.4199 [hep-ph]].
- [19] A. Arbey, M. Battaglia and F. Mahmoudi, Eur. Phys. J. C **72** (2012) 2169 [arXiv:1205.2557 [hep-ph]].
- [20] A. Fowlie, M. Kazana, K. Kowalska, S. Munir, L. Roszkowski, E. M. Sessolo, S. Trojanowski and Y. -L. S. Tsai, Phys. Rev. D **86** (2012) 075010 [arXiv:1206.0264 [hep-ph]].
- [21] M. W. Cahill-Rowley, J. L. Hewett, S. Hoeche, A. Ismail and T. G. Rizzo, Eur. Phys. J. C **72** (2012) 2156 [arXiv:1206.4321 [hep-ph]].
- [22] C. Beskidt, W. de Boer, D. I. Kazakov and F. Ratnikov, Eur. Phys. J. C **72** (2012) 2166 [arXiv:1207.3185 [hep-ph]].
- [23] M. W. Cahill-Rowley, J. L. Hewett, A. Ismail and T. G. Rizzo, “More Energy, More Searches, but the pMSSM Lives On,” arXiv:1211.1981 [hep-ph].
- [24] F. Mahmoudi, A. Arbey, M. Battaglia and A. Djouadi, “Implications of LHC Higgs and SUSY searches for MSSM,” arXiv:1211.2794 [hep-ph].
- [25] E. Aprile *et al.* [XENON100 Collaboration], Phys. Rev. Lett. **109** (2012) 181301 [arXiv:1207.5988 [astro-ph.CO]].
- [26] U. Ellwanger, C. Hugonie and A. M. Teixeira, Phys. Rept. **496** (2010) 1 [arXiv:0910.1785 [hep-ph]].
- [27] A. Arvanitaki and G. Villadoro, JHEP **1202** (2012) 144 [arXiv:1112.4835 [hep-ph]].
- [28] L. J. Hall, D. Pinner and J. T. Ruderman, JHEP **1204** (2012) 131 [arXiv:1112.2703 [hep-ph]].
- [29] U. Ellwanger, JHEP **1203** (2012) 044 [arXiv:1112.3548 [hep-ph]].
- [30] J. F. Gunion, Y. Jiang and S. Kraml, Phys. Lett. B **710** (2012) 454 [arXiv:1201.0982 [hep-ph]].
- [31] S. F. King, M. Muhlleitner and R. Nevzorov, Nucl. Phys. B **860** (2012) 207 [arXiv:1201.2671 [hep-ph]].
- [32] Z. Kang, J. Li and T. Li, JHEP **1211** (2012) 024 [arXiv:1201.5305 [hep-ph]].
- [33] J. -J. Cao, Z. -X. Heng, J. M. Yang, Y. -M. Zhang and J. -Y. Zhu, JHEP **1203** (2012) 086 [arXiv:1202.5821 [hep-ph]].

- [34] D. A. Vasquez, G. Belanger, C. Boehm, J. Da Silva, P. Richardson and C. Wymant, Phys. Rev. D **86** (2012) 035023 [arXiv:1203.3446 [hep-ph]].
- [35] U. Ellwanger and C. Hugonie, Adv. High Energy Phys. **2012** (2012) 625389 [arXiv:1203.5048 [hep-ph]].
- [36] K. S. Jeong, Y. Shoji and M. Yamaguchi, JHEP **1209** (2012) 007 [arXiv:1205.2486 [hep-ph]].
- [37] R. Benbrik, M. Gomez Bock, S. Heinemeyer, O. Stal, G. Weiglein and L. Zeune, Eur. Phys. J. C **72** (2012) 2171 [arXiv:1207.1096 [hep-ph]].
- [38] J. F. Gunion, Y. Jiang and S. Kraml, Phys. Rev. D **86** (2012) 071702 [arXiv:1207.1545 [hep-ph]].
- [39] J. Cao, Z. Heng, J. M. Yang and J. Zhu, JHEP **1210** (2012) 079 [arXiv:1207.3698 [hep-ph]].
- [40] T. Cheng, J. Li, T. Li, X. Wan, Y. k. Wang and S. -h. Zhu, “Toward the Natural and Realistic NMSSM with and without R -Parity,” arXiv:1207.6392 [hep-ph].
- [41] K. Schmidt-Hoberg and F. Staub, JHEP **1210** (2012) 195 [arXiv:1208.1683 [hep-ph]].
- [42] Z. Kang, T. Li, J. Li and Y. Liu, “A Radiatively Light Stop Saves the Best Global Fit for Higgs Boson Mass and Decays,” arXiv:1208.2673 [hep-ph].
- [43] G. Belanger, U. Ellwanger, J. F. Gunion, Y. Jiang and S. Kraml, “Two Higgs Bosons at the Tevatron and the LHC?,” arXiv:1208.4952 [hep-ph].
- [44] K. Agashe, Y. Cui and R. Franceschini, “Natural Islands for a 125 GeV Higgs in the scale-invariant NMSSM,” arXiv:1209.2115 [hep-ph].
- [45] G. Belanger, U. Ellwanger, J. F. Gunion, Y. Jiang, S. Kraml and J. H. Schwarz, JHEP **1301** (2013) 069 [arXiv:1210.1976 [hep-ph]].
- [46] Z. Heng, “A 125 GeV Higgs and its di-photon signal in different SUSY models: a mini review,” arXiv:1210.3751 [hep-ph].
- [47] K. Choi, S. H. Im, K. S. Jeong and M. Yamaguchi, “Higgs mixing and diphoton rate enhancement in NMSSM models,” arXiv:1211.0875 [hep-ph].
- [48] S. F. King, M. Muhlleitner, R. Nevzorov and K. Walz, “Natural NMSSM Higgs Bosons,” arXiv:1211.5074 [hep-ph].
- [49] T. Gherghetta, B. von Harling, A. D. Medina and M. A. Schmidt, “The Scale-Invariant NMSSM and the 126 GeV Higgs Boson,” arXiv:1212.5243 [hep-ph].
- [50] Z. Kang, J. Li, T. Li, D. Liu and J. Shu, “Probing the CP-even Higgs Sector via $H_3 \rightarrow H_2 H_1$ in the Natural NMSSM,” arXiv:1301.0453 [hep-ph].

- [51] U. Ellwanger, G. Espitalier-Noel and C. Hugonie, JHEP **1109** (2011) 105 [arXiv:1107.2472 [hep-ph]].
- [52] U. Ellwanger and C. Hugonie, Eur. Phys. J. C **5** (1998) 723 [hep-ph/9712300].
- [53] U. Ellwanger and C. Hugonie, Eur. Phys. J. C **13** (2000) 681 [hep-ph/9812427].
- [54] V. Barger, P. Langacker and G. Shaughnessy, Phys. Lett. B **644** (2007) 361 [hep-ph/0609068].
- [55] D. Das, U. Ellwanger and A. M. Teixeira, JHEP **1204** (2012) 067 [arXiv:1202.5244 [hep-ph]].
- [56] H. K. Dreiner, F. Staub and A. Vicente, “General NMSSM signatures at the LHC,” arXiv:1211.6987 [hep-ph].
- [57] J. F. Gunion, D. E. Lopez-Fogliani, L. Roszkowski, R. Ruiz de Austri and T. A. Varley, Phys. Rev. D **84** (2011) 055026 [arXiv:1105.1195 [hep-ph]].
- [58] S. Chatrchyan *et al.* [CMS Collaboration], Phys. Rev. D **85** (2012) 012004 [arXiv:1107.1279 [hep-ex]].
- [59] K. Kowalska, S. Munir, L. Roszkowski, E. M. Sessolo, S. Trojanowski and Y. - L. S. Tsai, “The Constrained NMSSM with a 125 GeV Higgs boson – A global analysis,” arXiv:1211.1693 [hep-ph].
- [60] S. Schael *et al.* [ALEPH and DELPHI and L3 and OPAL Collaborations and LEP Working Group for Higgs Boson Searches], Eur. Phys. J. C **47** (2006) 547 [arXiv:hep-ex/0602042].
- [61] U. Ellwanger and C. Hugonie, Comput. Phys. Commun. **177** (2007) 399 [hep-ph/0612134].
- [62] U. Ellwanger, J. F. Gunion and C. Hugonie, JHEP **0502** (2005) 066 [arXiv:hep-ph/0406215].
- [63] U. Ellwanger and C. Hugonie, Comput. Phys. Commun. **175** (2006) 290 [arXiv:hep-ph/0508022].
- [64] G. Degrandi and P. Slavich, Nucl. Phys. B **825** (2010) 119 [arXiv:0907.4682 [hep-ph]].
- [65] G. Belanger, F. Boudjema, C. Hugonie, A. Pukhov and A. Semenov, JCAP **0509** (2005) 001 [arXiv:hep-ph/0505142].
- [66] G. Belanger, F. Boudjema, A. Pukhov and A. Semenov, Comput. Phys. Commun. **176**, 367 (2007) [arXiv:hep-ph/0607059].
- [67] G. Belanger, F. Boudjema, A. Pukhov and A. Semenov, Comput. Phys. Commun. **180** (2009) 747 [arXiv:0803.2360 [hep-ph]].

- [68] G. Aad *et al.* [ATLAS Collaboration], “Search for top and bottom squarks from gluino pair production in final states with missing transverse energy and at least three b-jets with the ATLAS detector,” *Eur. Phys. J. C* **72** (2012) 2174 [arXiv:1207.4686 [hep-ex]].
- [69] G. Aad *et al.* [ATLAS Collaboration], “Search for supersymmetry in pp collisions at $\sqrt{s} = 7$ TeV in final states with missing transverse momentum and b-jets with the ATLAS detector,” *Phys. Rev. D* **85** (2012) 112006 [arXiv:1203.6193 [hep-ex]].
- [70] G. Aad *et al.* [ATLAS Collaboration], “Search for a supersymmetric partner to the top quark in final states with jets and missing transverse momentum at $\sqrt{s} = 7$ TeV with the ATLAS detector,” *Phys. Rev. Lett.* **109** (2012) 211802 [arXiv:1208.1447 [hep-ex]].
- [71] G. Aad *et al.* [ATLAS Collaboration], “Search for direct top squark pair production in final states with one isolated lepton, jets, and missing transverse momentum in $\sqrt{s} = 7$ TeV *pp* collisions using 4.7 fb^{-1} of ATLAS data,” *Phys. Rev. Lett.* **109** (2012) 211803 [arXiv:1208.2590 [hep-ex]].
- [72] G. Aad *et al.* [ATLAS Collaboration], “Search for light top squark pair production in final states with leptons and b-jets with the ATLAS detector in $\sqrt{s} = 7$ TeV proton-proton collisions,” arXiv:1209.2102 [hep-ex].
- [73] G. Aad *et al.* [ATLAS Collaboration], “Search for a heavy top-quark partner in final states with two leptons with the ATLAS detector at the LHC,” *JHEP* **1211** (2012) 094 [arXiv:1209.4186 [hep-ex]].
- [74] CMS Collaboration, “Search for supersymmetry in final states with missing transverse energy and 0, 1, 2, or ≥ 3 b jets in 7 TeV pp collisions”, CMS-PAS-SUS-11-022
- [75] X. -J. Bi, Q. -S. Yan and P. -F. Yin, “Light stop/sbottom pair production searches in the NMSSM,” arXiv:1209.2703 [hep-ph].
- [76] J. Alwall, M. Herquet, F. Maltoni, O. Mattelaer and T. Stelzer, *JHEP* **1106** (2011) 128 [arXiv:1106.0522 [hep-ph]].
- [77] T. Sjostrand, S. Mrenna and P. Z. Skands, *JHEP* **0605** (2006) 026 [hep-ph/0603175].
- [78] J. Alwall, S. de Visscher and F. Maltoni, *JHEP* **0902** (2009) 017 [arXiv:0810.5350 [hep-ph]].
- [79] D. Das, U. Ellwanger and A. M. Teixeira, *Comput. Phys. Commun.* **183** (2012) 774 [arXiv:1106.5633 [hep-ph]].
- [80] M. Muhlleitner, A. Djouadi and Y. Mambrini, *Comput. Phys. Commun.* **168** (2005) 46 [arXiv:hep-ph/0311167].
- [81] S. Ovin, X. Rouby and V. Lemaitre, “DELPHES, a framework for fast simulation of a generic collider experiment,” arXiv:0903.2225 [hep-ph].
- [82] M. Cacciari, G. P. Salam and G. Soyez, *JHEP* **0804** (2008) 063 [arXiv:0802.1189 [hep-ph]].

- [83] M. Cacciari and G. P. Salam, Phys. Lett. B **641** (2006) 57 [arXiv:hep-ph/0512210].
- [84] W. Beenakker, R. Hopker, M. Spira and P. M. Zerwas, Nucl. Phys. B **492** (1997) 51 [arXiv:hep-ph/9610490].
- [85] W. Beenakker, R. Hopker and M. Spira, “PROSPINO: A program for the PROduction of Supersymmetric Particles In Next-to-leading Order QCD,” arXiv:hep-ph/9611232, for updates see <http://www.thphys.uni-heidelberg.de/~plehn/prospino/>
- [86] W. Beenakker, M. Klasen, M. Kramer, T. Plehn, M. Spira and P. M. Zerwas, Phys. Rev. Lett. **83** (1999) 3780 [Erratum-ibid. **100** (2008) 029901] [arXiv:hep-ph/9906298].
- [87] W. Beenakker, S. Brensing, M. Kramer, A. Kulesza, E. Laenen, L. Motyka and I. Niessen, Int. J. Mod. Phys. A **26** (2011) 2637 [arXiv:1105.1110 [hep-ph]].
- [88] M. Kramer, A. Kulesza, R. van der Leeuw, M. Mangano, S. Padhi, T. Plehn and X. Portell, “Supersymmetry production cross sections in pp collisions at $\sqrt{s} = 7$ TeV,” arXiv:1206.2892 [hep-ph].